The β5′ Loop of the Pancreatic Lipase C2-like Domain Plays a Critical Role in the Lipase−Lipid Interactions†

Henri Chahinian,‡ Sofiane Bezzine,‡ Francine Ferrato,‡ Margarita G. Ivanova,‡ Barbara Perez,‡ Mark E. Lowe,§ and Frédéric Carrière*,‡

Laboratoire de Lipolyse Enzymatique du CNRS, 31 chemin Joseph Aiguier, 13402 Marseille cedex 20, France, and Departments of Pediatrics and of Molecular Biology and Pharmacology, Washington University School of Medicine and St. Louis Children's Hospital, St. Louis, Missouri 63110

Received March 11, 2002; Revised Manuscript Received May 6, 2002

ABSTRACT: The structural similarities between the C-terminal domain of human pancreatic lipase (C-HPL) and C2 domains suggested a similar function, the interaction with lipids. The catalytic N-terminal domain (N-HPL) and C-HPL were produced as individual proteins, and their partitioning between the water phase and the triglyceride−water interface was assessed using trioctanoin emulsions (TC8). N-HPL did not bind efficiently to TC8 and was inactive. C-HPL did bind to TC8 and to a phospholipid monolayer with a critical surface pressure of penetration similar to that of HPL (15 mN m^{-1}). These experiments, performed in the absence of colipase and bile salts, support an absolute requirement of C-HPL for interfacial binding of HPL. To refine our analysis, we determined the contribution to lipid interactions of a hydrophobic loop (β5′) in C-HPL by investigating a HPL mutant in which β5′ loop hydrophobicity was increased by introducing the homologous lipoprotein lipase (LPL) β5′ loop. This mutant (HPL-β5′LPL) penetrated into phospholipid monolayers at higher surface pressures than HPL, and its level of binding to TC8 was higher than that of HPL in the presence of serum albumin (BSA), an inhibitory protein that competes with HPL for interfacial adsorption. The β5′ loop of LPL is therefore tailored for an optimal interaction with the surface of triglyceride-rich lipoproteins (VLDL and chylomicrons) containing phospholipids and apoproteins. These observations support a major contribution of the β5′ loop in the interaction of LPL and HPL with their respective substrates.

The three-dimensional (3D) structure of pancreatic lipase (PL)[1] consists of two functional domains. The N-terminal domain belongs to the α/β hydrolase fold family of proteins and contains the active site, which involves a catalytic triad analogous to that present in serine proteases. A surface loop (C237−C261) in the N-terminal domain forms the so-called lid, which controls the access of substrate to the active site (*1*, *2*). The β-sandwich C-terminal domain (residues 336−449) of PL plays an important part in the binding of PL and colipase, a protein cofactor for PL (*3*). The presence of the noncatalytic C-terminal domain of ∼100 residues distinguishes PL from all the other triglyceride lipases for which the 3D structures have been determined. Other enzymes belonging to the pancreatic lipase gene family such as hepatic lipase (HL), lipoprotein lipase [LPL (*4*)], endothelial lipase [EL (*5*)], phosphatidylserine-specific phospholipase A1 [PS-PLA1 (*6*)], and pancreatic lipase-related proteins (*7*, *8*) also contain a C-terminal domain.

Recent structure−function studies have suggested that the C-terminal domain of PL may have another role apart from that of binding colipase (*9*). The distal part of the C-terminal domain contains an exposed hydrophobic loop (β5′ loop, residues 405−414 between β-strands β5′ and β6′) which resides on the same side as the hydrophobic loops surrounding the active site (Figure 1A), and it may be involved in the lipid binding process. The β5′ loop exhibits a large accessible surface area (877 $Å^2$), which is significantly apolar with 488 $Å^2$ occupied by hydrophobic side chains. Moreover, colipase binding does not mask the hydrophobic surface of the β5′ loop (Figure 1B), and when colipase binds, the β5′ loop forms a large hydrophobic plateau with the open lid, the β9 loop, and the tips of the colipase fingers (Figure 1B,C). This orientation of the β5′ loop places the loop in position to participate in lipid binding.

Studies with LPL suggest that a loop in a position homologous to the β5′ loop of PL contributes to the lipid

† This work was supported by European Union BIOTECH G programmes BIO2-CT94-3013 and BIO2-CT94-3041 and by NIH Grants HD330600 and DK52574.

* To whom correspondence should be addressed: Laboratoire de Lipolyse Enzymatique du CNRS, 31 chemin Joseph Aiguier, 13402 Marseille cedex 20, France. Telephone: (33) 4 91 16 41 92. Fax: (33) 4 91 71 58 57. E-mail: carriere@ibsm.cnrs-mrs.fr.

‡ Laboratoire de Lipolyse Enzymatique du CNRS.

§ Washington University School of Medicine and St. Louis Children's Hospital.

[1] Abbreviations: AcMNPV, *A. californica* multinuclear polyhedrosis virus; BSA, bovine serum albumin; CBR, calcium binding region; C-HPL, C-terminal domain of human pancreatic lipase; cPLA2, cytosolic phospholipase A2; EL, endothelial lipase; EPR, electron paramagnetic resonance; FPLC, fast protein liquid chromatography; HL, hepatic lipase; HPL, human pancreatic lipase; HPL-β5′LPL, human pancreatic lipase mutant in which the β5′ loop has been substituted with that of LPL; HPL S152G, HPL mutant in which the active site serine 152 has been substituted with a glycine residue; LPL, lipoprotein lipase; mAb, monoclonal antibody; MALDI-TOF, matrix-assisted laser desorption ionization time of flight; NaTDC, sodium taurodeoxycholate; N-HPL, N-terminal domain of human pancreatic lipase; PC, phosphatidylcholine; PL, pancreatic lipase; PS-PLA1, phosphatidylserine-specific phospholipase A1; TC8, trioctanoin; VLDL, very low-density lipoproteins.

10.1021/bi0257944 CCC: $22.00
Published on Web 10/24/2002

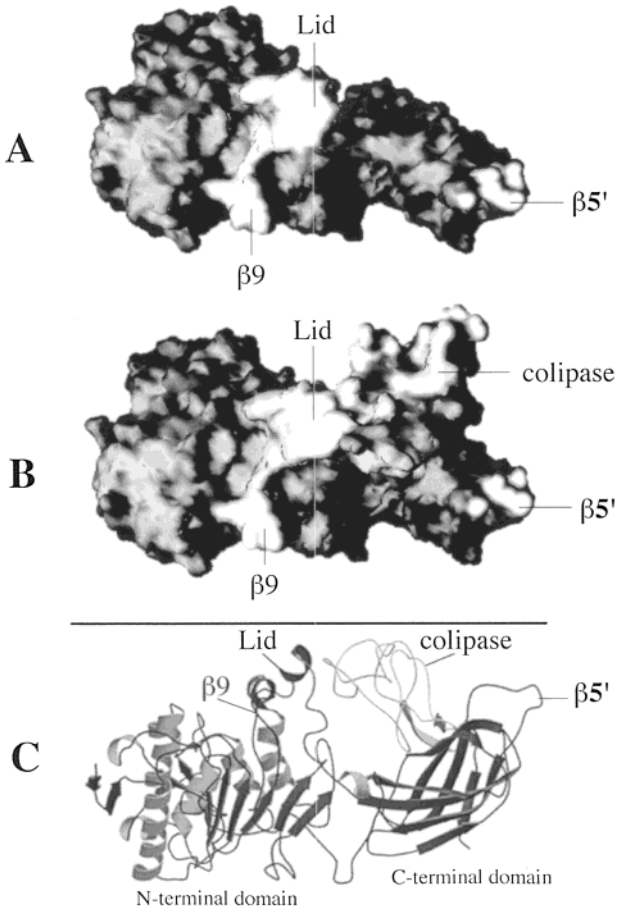

FIGURE 1: Tentative model for the adsorption of the pancreatic lipase−colipase complex at a lipid−water interface. (A) Molecular surface representation of the open conformation of the HPL 3D structure. The hydrophobic surfaces are indicated in white. (B) Molecular surface representation of the open HPL−colipase complex. (C) Side view of the HPL−colipase complex represented as a ribbon model. The lid domain, the β9 loop, and the β5′ loop of HPL are defining a plane that might be aligned with the lipid−water interface (A and C). In the pancreatic lipase−colipase complex, the hydrophobic tips of colipase fingers are also found on the same plane (B and C). All together, the lipase and colipase residues located on this plane constitute a large hydrophobic surface that confers an amphiphilic character to the pancreatic lipase−colipase complex. Molecular surfaces were generated using GRASP (*50*), and the ribbon 3D model was obtained using Molscript (*51*) and Raster 3D (*52*).

binding of LPL (*10*, *11*). A monoclonal antibody (5D2) that interacts with this loop in LPL inhibited LPL activity (Figure 2). Moreover, proteolytic cleavage within the LPL β5′ loop decreased activity against long chain triglyceride emulsions and chylomicrons without affecting the activity against the soluble substrates (*12*). Finally, mutagenesis of three tryptophans in the LPL loop abolished the binding of the lipase to lipoproteins (*11*). These three tryptophan residues (W390, W393, and W394; see Figure 2) increase the hydrophobicity of the longer LPL β5′ loop compared to that of the β5′ loop in PL.

Other observations suggest that the C-terminal domain of PL may interact directly with the oil−water interface. Studies with monoclonal antibodies directed against the β5′ loop provide indirect evidence for a role of the C-terminal domain of PL in lipid binding. The formation of PL−antibody complexes drastically reduced the catalytic activity against emulsified water insoluble substrates, whereas the activity

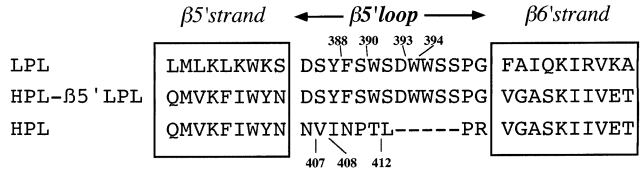

FIGURE 2: Sequence alignments in the region of the β5′ loop. The β5′ and β6′ strands of the HPL C-terminal domain were aligned with the corresponding β-strands of human LPL based on sequence homologies. The amino acid residues and the size of the β5′ loop connecting these two β-strands are not conserved in LPL and HPL, but the two loops contain hydrophobic residues that are essential for the interactions with lipids or detergents [W390, W393, and W394 in LPL (*11*) and I408−L412 in porcine pancreatic lipase (*14*)]. All these hydrophobic residues are found to be exposed at the surface of the molecule in the X-ray structure of HPL (*1*), as well as in the 3D homology model of LPL (*4*). The entire LPL β5′ loop was substituted with the HPL β5′ loop in the HPL-β5′LPL mutant.

of these complexes on a soluble substrate remained unchanged (*9*). An HPL mutant (N-HPL) devoid of the C-terminal domain displayed some activity toward the partly soluble tripropionin, but not toward a trioctanoin emulsion (*9*). Studies on the stability of PL mutants at oil−water interface showed that the interfacial denaturation of HPL depends on the nature of the C-terminal domain (*13*). In addition, a study of the PL−colipase complex by neutron diffraction crystallography revealed that a micelle of nonionic detergent (tetraethylene glycol monooctyl ether) can interact with colipase and with the distal part of the C-terminal domain of PL, including several residues (I408−L412) from the β5′ loop (*14*). This later study demonstrated the ability of the β5′ loop to interact with aggregated amphiphilic molecules.

During the past few years, the protein structures of 15-lipoxygenase (*15*) and *Clostridium perfringens* α-toxin (*16*) revealed that both contain a domain that is closely structurally homologous to the β-sandwich C-terminal domain of PL. Generally speaking, these domains show structural homologies with the C2 domains occurring in a wide range of proteins involved in signal transduction (e.g., phosphoinositide-specific phospholipase C, protein kinase C, and cytosolic phospholipase A2), membrane trafficking (e.g., synaptotagmin I and rabphilin), and membrane disruption (e.g., perforin) (*17*, *18*). Like the C-terminal domain of PL, the C2 domains show a β-sandwich structure with three hydrophobic loops (CBRs 1−3). Additionally, a calcium binding region resides on the same side of the domain as do the hydrophobic loops. Both hydrophobic residues and calcium ions are essential for the interaction of C2 domains with phospholipid vesicles, and these domains are often named calcium-dependent lipid binding domains. When the C-terminal domain of PL is superimposed on the C2 domain of cytosolic phospholipase A2 (cPLA2), one can see that the β-strand connectivity is not the same and that the calcium binding site is not conserved in PL. Still, the β5′ loop of PL has the same topology as the CBR3 hydrophobic loop (*19*). Strikingly, the β5′ loop of PL and the CBR3 loop are both located on the same face of the molecule as the active site covered by a lid (*20*).

Similarly, a short loop with the same topology as the β5′ loop of PL is observed in the C2-like domain of mammalian lipoxygenases. This loop also contains hydrophobic amino

Table 1: Primers Used for PCR Mutagenesis

	primer sequence and comments
1	CCC ACA GGG GGA TCC GCT CGG CAT, sense primer annealing to HPL cDNA 5′ end (*Bam*HI underlined)
2	CCG GAA TTC TCA GCA GGG TGT CAG CG, antisense primer annealing to HPL cDNA 3′ end (*Eco*RI underlined)
3	**AGC TGG TCA GAC TGG TGG AGC AGT CCC GGG** GTG GGA GCA TCC AAG ATT, sense primer annealing with HPL cDNA downstream of the β5′ loop and encoding the SWSDWWSSPG residues (**bold nucleotides**) present in the β5′ loop of HPL-β5′LPL (*Sma*I underlined)
4	**CCA CCA GTC TGA CCA GCT AAA GTA TGA ATC** GTT ATA CCA AAT AAA TTT AAC C, antisense primer annealing with HPL cDNA upstream of the β5′ loop and encoding the DSYFSWSDWW residues (**bold nucleotides**) present in the β5′ loop of HPL-β5′LPL

acid residues (F70 and L71 in 15-lipoxygenase) which are located on the same face of the molecule as the active site (*15*). The hydrophobic character of these surface residues is conserved in all lipoxygenases, and it was suggested that they play a critical role in localizing lipoxygenases near their substrates in membranes or lipoproteins (*15*). It was recently demonstrated that the C2-like domain of 5-lipoxygenase is required and sufficient for nuclear membrane translocation in human embryonic kidney cells (*21*).

In the study presented here, we first produced the N- and C-terminal domains of PL as individual proteins and investigated their ability to interact with lipids. We then focused on the β5′ loop of the C-terminal domain, and we investigated whether the hydrophobicity of the PL β5′ loop influenced the interfacial binding and activity of pancreatic lipase. For this purpose, we produced and characterized a HPL mutant in which the hydrophobicity of the β5′ loop was increased by introducing the LPL β5′ loop (HPL-β5′LPL mutant). The mutant was expressed in insect cells and purified to homogeneity prior to being kinetically characterized using emulsions of water insoluble trioctanoin and phospholipid monomolecular films. The effects of bile salts, colipase, and bovine serum albumin (BSA) on the interfacial binding of the HPL-β5′LPL mutant were studied and compared to the properties of HPL.

EXPERIMENTAL PROCEDURES

DNA Source and Manipulations. A 1411 bp cDNA encoding HPL was previously obtained from human placenta mRNA (*22*, *23*). All plasmids were produced and amplified in *Escherichia coli* after electroporation of ElectroMAX DH10B cells (Life Technologies). Plasmid DNAs were isolated from *E. coli* cultures using the alkaline lysis procedure (*24*) and purified using the Wizard DNA purification system (Promega). Digestion with restriction enzymes and ligation with T4 DNA ligase were performed as recommended by the enzyme supplier (New England Biolabs). DNA sequencing was performed by Genome Express (Grenoble, France).

Site-Directed Mutagenesis. Point mutations were performed using the PCR overlap extension technique (*25*) with internal oligonucleotides carrying the specific mutations, and two external oligonucleotides corresponding to the 5′ and 3′ ends of HPL cDNA, respectively. These later primers introduced *Bam*HI and *Eco*RI restriction sites for further subcloning of the PCR products into the pVL1393 baculovirus transfer vector. PCRs were carried out using *pfu* DNA polymerase (Stratagene).

HPL-β5′LPL Mutant. The first PCR was carried out using HPL cDNA in pVL1392 as the template (1411 bp *Bam*HI DNA fragment subcloned in the pVL1392 vector) and primers 1 and 4 (Table 1), for 30 cycles of 1 min at 94 °C, 2 min at 54 °C, and 3 min at 72 °C. The second PCR was carried out using HPL cDNA in pVL1392 as the template and primers 2 and 3 (Table 1), for 30 cycles of 1 min at 94 °C, 2 min at 54 °C, and 3 min at 72 °C. The third PCR ligation−amplification step was carried out using the products of PCR 1 and PCR 2 as the templates, and primers 1 and 2 for 30 cycles of 1 min at 94 °C, 2 min at 54 °C, and 3 min at 72 °C. To help identify mutated inserts, a new *Sma*I restriction site was introduced into HPL cDNA by primer 3. The PCR3 product was digested by *Bam*HI and *Eco*RI, and the resulting DNA fragment was subcloned into the pVL1393 baculovirus transfer vector (Invitrogen).

Production of the HPL-β5′LPL Mutant Using the Baculovirus Expression System. Recombinant baculovirus production and HPL mutant expression were performed as previously described (*26*). The pVL1393 baculovirus transfer vectors containing the mutated HPL cDNAs were used for the cotransfection of Sf9 insect cells (*Spodoptera frugiperda*) with the linearized genomic DNA from *Autographa californica* baculovirus (AcMNPV from the BaculoGold transfection kit, Pharmingen). The Sf9 cells were grown in monolayers at 27 °C in tissue culture flasks, using TNM-FH medium (Sigma) supplemented with 10% fetal calf serum (Bio-Whittaker) and a 1% antibiotic−antimycotic solution (Gibco BRL-Life Technologies) containing 10 000 units/mL penicillin G, 10 000 μg/mL streptomycin, and 25 μg/mL amphotericin B (Fungizone). The insect cell cotransfection was performed using 1 μg of linear AcMNPV DNA and 3 μg of the recombinant pVL1393 mixed with cationic liposomes, and added to a 60 mm Petri dish containing 2×10^6 Sf9 cells grown in TNM-FH medium. The culture supernatants were collected after the lysis of all the cells (approximately 7 days postinfection), and were used as the primary stocks of the recombinant baculovirus expressing the HPL mutant. An additional stage of cell infection was performed to amplify the viruses and generate the high-titer virus stocks (10^7-10^9 pfu/mL or plaque-forming units per milliliter of culture) required for recombinant protein production. The virus titers were estimated using the end-point dilution assay method as previously described (*27*). The production of the HPL-β5′LPL mutant was carried out using another cell line from *Trichoplusia ni*, grown in a monolayer at densities of up to 5×10^7 cells per 175 cm^2 culture flask, in 25 mL of EX-CELL 400 medium (JRH-Biosciences) supplemented with the previously mentioned antibiotic−antimycotic solution (0.5%). An inoculum of each recombinant baculovirus encoding an HPL mutant was added to the cell culture at a multiplicity of infection of ∼10 pfu/

cell. Six hours postinfection, the culture supernatant was removed by aspiration and replaced with 25 mL of fresh EX-CELL 400 medium. The baculovirus-infected insect cell cultures were harvested 2 or 3 days after the infection to prevent any intracellular proteases released upon cell lysis from degrading the recombinant protein.

Purification of the HPL-β5′LPL Mutant. The HPL-β5′LPL mutant was purified using the one-step procedure previously developed for the purification of HPL expressed in insect cells (*22*). The culture medium was centrifuged at 10 000 rpm for 10 min, and the supernatant was lyophilized for 24 h. The dry material was dissolved in a few milliliters of distilled water and dialyzed overnight against 10 mM MES buffer (pH 6.5). Prior to chromatography, the solution was run through a 0.8 μm Millipore filter. Using FPLC (Pharmacia), cation exchange chromatography was performed on a Mono S HR 5/5 column equilibrated in 10 mM MES buffer (pH 6.5). After each sample had been injected, a linear NaCl concentration gradient was applied from 0 to 100 mM NaCl, within 60 min. The flow rate was adjusted to 1 mL/min. The protein elution profile was recorded spectrophotometrically at 280 nm, and the lipase activity was measured potentiometrically in all the fractions collected using the pHstat technique and tributyrin as the substrate (see Lipase Activity Measurements). The main fractions containing lipase activity were subjected to 12% SDS−PAGE analysis (*28*), and those displaying a single protein band at 50 kDa were pooled and concentrated. The protein concentrations were estimated by performing amino acid analysis as well as a specific HPL ELISA.

Hydrophobic Interaction Chromatography. Samples of purified HPL and HPL-β5′LPL were subjected to hydrophobic interaction chromatography on 2.5 mL alkyl-agarose columns (Sigma) at room temperature. A preliminary screening of binding and elution of HPL mutant was performed using ethyl-, propyl-, butyl-, hexyl-, octyl-, decyl-, and dodecylagarose columns and an elution buffer [10 mM Tris-HCl (pH 7.5)] containing various NaCl concentrations. The decylagarose column was the only one for which the lipases could be retained and further eluted by decreasing the NaCl concentration. The final conditions for comparing the hydrophobic interactions of HPL and HPL-β5′LPL were as follows. Using an FPLC system (Pharmacia), hydrophobic interaction chromatography was performed on a 2.5 mL decylagarose column equilibrated in 10 mM Tris-HCl (pH 7.5) containing either 0.1 or 1 M NaCl, with a flow rate adjusted to 0.4 mL/min. After injection of the lipase sample (20−60 μg), the protein elution profile was recorded spectrophotometrically at 280 nm and the lipase activity was measured potentiometrically in all the fractions that were collected using the pHstat technique and tributyrin as the substrate (see Lipase Activity Measurements).

Structural Characterization of the HPL-β5′LPL Mutant. Samples of the purified HPL-β5′LPL mutant were subjected to N-terminal amino acid sequencing by automated Edman degradation using an Applied Biosystems model 473A gas-phase sequencer. Mass determination was performed by MALDI-TOF mass spectrometry using Voyager DE-RP equipment (Perspective Biosystems Inc.).

Production and Purification of N-HPL and C-HPL. Recombinant N-HPL was produced in insect cells, and C-HPL was obtained by performing limited chymotryptic cleavage of the recombinant HPL as previously described (*9*). C-HPL (14 kDa) was further purified from the proteolytic mixture by gel filtration chromatography using an Ultrogel AcA-54 column (1.5 cm × 200 cm). C-HPL could bind colipase, and it was therefore assumed that C-HPL retained its 3D structure.

Lipase Activity Measurements. The lipase activity of HPL was assayed in bulk by assessing the release of fatty acids from mechanically stirred emulsions of trioctanoin or tributyrin (puriss grade from Fluka). Using a pHstat apparatus (TTT 80 radiometer), the free fatty acids were automatically titrated with 0.1 N NaOH at a constant pH value of 7.5. Each reaction was performed in a 50 mL thermostated vessel (37 °C) containing 0.25 mL of substrate and 15 mL of 0.28 mM Tris-HCl buffer, 150 mM NaCl, and 1.4 mM $CaCl_2$, as well as variable concentrations of sodium taurodeoxycholate (NaTDC) or bovine serum albumin (BSA) when required. For routine assays, a NaTDC concentration of 0.5 mM was used. When required, pure colipase from porcine pancreas was added at a molar excess of 5. The lipolytic activities are expressed here in international units (U) per milligram of enzyme. One unit corresponds to 1 μmol of fatty acid released per minute.

Binding of HPL and the HPL-β5′LPL Mutant to Trioctanoin Emulsions. The interfacial binding of HPL was assayed by mixing the enzyme with a trioctanoin emulsion formed in a pHstat vial by mechanical stirring, and by further measuring the lipase activity remaining in the water phase after the separation of the oil phase (*29*). A pHstat vial thermostated at 37 °C was filled with 0.25 mL of trioctanoin (puriss grade from Sigma, St. Quentin-Fallavier, France) and 15 mL of 0.28 mM Tris-HCl buffer, 150 mM NaCl, and 1.4 mM $CaCl_2$, containing various concentrations of either NaTDC or BSA (Sigma). The vial was placed on the automatic titrator (TTT 80 radiometer), and its contents were stirred mechanically for 5 min to obtain a fine trioctanoin emulsion and to monitor the pH value at 7.5 by addition of 0.1 N NaOH. When required, colipase was added during this 5 min period. The HPL or mutant (10 μg, 200 pmol) was then added to the emulsion, and after incubation for 2 min, the contents of the pHstat vial were transferred into a puncturable 25 mm × 64 mm centrifuge tube (Beckman Ultra-Clear), which was kept on the bench for 1 h to obtain a satisfactory phase separation. After creaming had been carried out, a sample (1−2 mL) of the clear aqueous phase was recovered by introducing a 0.8 mm × 40 mm needle equipped with a 5 mL syringe into the bottom of the tube. The amount of lipase remaining in solution was determined either by measuring the residual lipase activity (*29*) or by performing an ELISA. For each reaction condition (with or without NaTDC, with or without BSA, and with or without colipase), a control experiment was performed without trioctanoin (0% binding) to check the recovery of the protein from the water phase. Before each experiment, the pHstat vial was washed successively with acetone, ethanol, and Milli-Q water to remove any trace of surface active compound that might modify the emulsion stability or impair protein recovery.

ELISA Protocols. A double-sandwich ELISA was performed to measure the amount of HPL, N-HPL, and HPL-β5′LPL remaining in the aqueous phase during the interfacial binding experiments. As previously reported (*30*), rabbit anti-

HPL polyclonal antibodies were used as capture antibodies, and the detector antibody was a mouse anti-HPL monoclonal antibody (mAb 146-40) that recognized an epitope in the HPL N-terminal domain.

A second double-sandwich ELISA procedure was established to measure the amount of C-HPL remaining in the aqueous phase during the interfacial binding experiments. Rabbit anti-HPL polyclonal antibodies were still used as capture antibodies, but the detector antibody was a mouse anti-HPL monoclonal antibody (mAb 315) that recognized an epitope in the HPL C-terminal domain. Using proteolytic cleavage, this conformational epitope was previously localized at the level of the β5′ loop (*9*). The mutagenesis of the β5′ loop performed in this study confirmed the localization of this epitope: the HPL-β5′LPL mutant was not recognized by mAb 315 (data not shown).

Monolayer Experiments. Using the monolayer technique, the kinetics of adsorption of HPL, C-HPL, and HPL-β5′LPL were studied by recording the changes with time of the surface pressure of a monomolecular film of egg phosphatidylcholine (PC) (Sigma) spread at the air−water interface in a cylindrical Teflon trough (volume, 5 mL; surface area, 7 cm^2). The surface pressure was measured using the Wilhelmy method with a thin platinum plate (perimeter, 3.94 cm) attached to an electromicrobalance (Beckman LM 600). The trough was filled with 10 mM Tris-HCl buffer (pH 8.0), 100 mM NaCl, 21 mM $CaCl_2$, and 1 mM EDTA, and the monolayer was spread using various volumes (1−10 μL) of a 1 mg/mL PC solution in chloroform. Once the initial surface pressure had stabilized, the lipase (5 μg, overall concentration in the trough of 20 nM) was injected into the aqueous subphase, which was stirred for 30 s at 250 rpm with a magnetic rod to homogenize the aqueous phase. The increase in the surface pressure was then recorded for 60 min. When the adsorption of C-HPL was being studied, 1.25 μg of C-HPL (molecular mass of 12 kDa) was injected under the monomolecular film to keep the same molarity (20 nM) as in the experiments performed with HPL.

Modeling of β5′ Loop Mutations and Calculating the Water Accessible Surfaces. A 3D model of the HPL-β5′LPL mutant was built after the superimposition of the X-ray 3D structure of open HPL (*2*) with the 3D model of human LPL (*4*) using Turbo-Frodo software (*31*). The HPL β5′ loop was deleted, and a new loop was built using the LPL β5′ loop as a template. The water accessible surfaces of the HPL-β5′LPL 3D model were calculated using the DSSP option (*32*) in Turbo-Frodo software.

RESULTS

Interfacial Binding of N- and C-HPL. The interfacial binding of the N- and C-terminal domains of HPL was studied using a trioctanoin emulsion and various bile salt concentrations (Table 2). After incubation of known amounts of protein [either 7.5 μg of N-HPL or 2.5 μg of C-HPL (13 nM each)] with the trioctanoin emulsion and a subsequent oil−water phase separation, the amounts of protein remaining in the water phase were quantitated by an ELISA. N-HPL bound weakly to the lipid−water interface, with a maximum level of binding of 26.0 ± 7.1% in the presence of 0.5 mM NaTDC. It was checked that the protein present in the water phase retained some activity on the partly soluble tripropionin substrate (*9*), suggesting that N-HPL was not unfolded (data not shown). On the other hand, C-HPL bound completely to the interface (99.4 ± 0.3%) in the absence of bile salts. It was not possible to check whether C-HPL was unfolded, and to what extent interfacial denaturation might have affected the binding to lipids. In the presence of bile salts, the ELISA measurements of C-HPL were poorly reproducible and could not be interpreted. The ELISA procedure involved a monoclonal antibody (mAb 315) recognizing the HPL β5′ loop (*9*), and this interaction was probably weakened or abolished by bile salts since micelles are known to interact with the HPL β5′ loop (*14*). Similar experiments were performed in the presence of colipase, and the interfacial binding of N-HPL and C-HPL was not found to be significantly different from that obtained in the absence of colipase (data not shown).

Table 2: Interfacial Binding of N-HPL and C-HPL at Various NaTDC Concentrations[a]

protein	[NaTDC] (mM)	binding (%)
N-HPL	0	15.4 ± 2.9
	0.5	26.0 ± 7.1
	4	6.8 ± 4.9
C-HPL	0	99.4 ± 0.3
	0.5	nd[b]
	4	nd[b]

[a] Experiments were performed using either 7.5 μg of N-HPL or 2.5 μg of C-HPL to keep the molarity (13 nM) the same as in the binding experiments performed with 10 μg of HPL (see Table 4). [b] Not determined.

We next determined the ability of C-HPL to bind and to penetrate a phospholipid monolayer using the monomolecular film technique. When C-HPL was injected under a film of phosphatidylcholine (PC), the increase in surface pressure was similar to that observed with full-length HPL, for initial surface pressures between 8 and 15 mN/m (Figure 3). No significant increase in surface pressure was recorded above 15 mN/m, revealing that C-HPL, like HPL, does not penetrate into the PC film above this critical surface pressure. For lower initial surface pressures (<5 mN/m), the adsorption of C-HPL onto the PC film induced an increase in surface pressure that was 2−3-fold lower than that observed with HPL (Figure 3).

Design, Expression, Purification, and Structural Analysis of the HPL-β5′LPL Mutant. The HPL-β5′LPL mutant was designed to increase the hydrophobicity of the β5′ loop. The β5′ loop of HPL (N406-VINPTLP-R414) was replaced with the longer loop observed in LPL at the same position (Figure 2). Starting from HPL cDNA as the template, we obtained the mutated DNA construct using the PCR overlap extension method and the specific primers listed in Table 1.

The DNA construct was subcloned into a baculovirus expression vector for production of the corresponding recombinant protein in insect cells. The HPL-β5′LPL mutant was secreted into the serum-free culture medium of insect cells (10−40 mg of recombinant protein per liter) and was purified to homogeneity using a single step of cation exchange chromatography as previously described in the case of recombinant HPL (*22*). After purification, the HPL-β5′LPL mutant was sequenced at the N-terminus to confirm the correct cleavage of the HPL signal peptide and to ensure that the recombinant protein had not been proteolytically

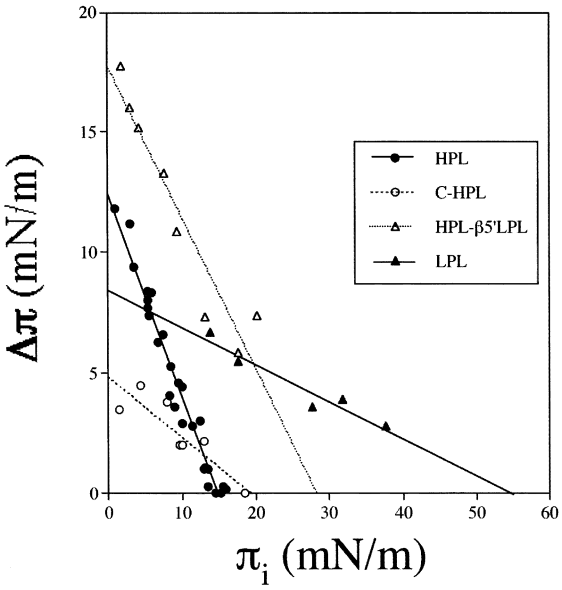

FIGURE 3: Comparison of HPL, HPL C-terminal domain, LPL, and HPL-β5′LPL adsorptions onto a monomolecular film of egg PC spread at the air−water interface. After the protein had been injected into the subphase, the maximum increase in the surface pressure ($\Delta\pi$) was plotted as a function of the initial surface pressure (π_i) of the egg PC monolayer. Both $\Delta\pi$ and π_i are expressed in millinewtons per meter. The linear curves describing $\Delta\pi = f(\pi_i)$ were obtained by linear regression using the least-squares method. The data on HPL and LPL adsorptions were previously reported in refs *29* and *33*, respectively.

cleaved. With this analysis and subsequent SDS−PAGE, we discovered that the HPL-β5′LPL mutant was cleaved into two polypeptides (approximately 46 and 4 kDa) with hydrolysis occurring after F388 in the LPL β5′ loop (Figure 2) of the HPL mutant. Because the degradation depended on the time of culture after viral infection, we harvested the recombinant protein 2 days postinfection. At this time, the HPL-β5′LPL mutant was intact. After purification, the molecular mass of the mutant was determined experimentally using MALDI-TOF mass spectrometry. A mass of 51 467 ± 12 Da was measured for HPL-β5′LPL. This experimental mass was ~1100−1200 Da greater than the theoretical mass of the polypeptide (50 203 Da). The presence of a short glycan chain, as we previously observed in recombinant HPL produced by insect cells, provides a plausible explanation for the difference (*22*).

Based on the 3D structure of HPL (*2*) and a 3D model of human LPL (*4*), a 3D model of HPL-β5′LPL was constructed (Figure 4). The water accessible surface of the β5′ loop residues was determined in each case and compared to that observed in the HPL β5′ loop (Table 3). The insertion of the larger LPL β5′ loop in HPL-β5′LPL doubled the total accessible surface (1529 vs 877 Å^2 in HPL), and the hydrophobic surface was increased from 488 Å^2 in HPL to 914 Å^2 in HPL-β5′LPL. Even so, the hydrophilic/lipophilic balance (HLB) was only slightly decreased because charged, semipolar, and hydrophobic surfaces were all increased proportionately (Table 3). It is worth noticing however that four "polar-aromatic" residues were introduced into HPL-β5′LPL, and they significantly contributed to the exposed hydrophobic surface (665 Å^2 out of 914 Å^2).

Effects of the β5′ Loop Mutation on the Hydrophobic Interactions. Samples of purified HPL and HPL-β5′LPL were

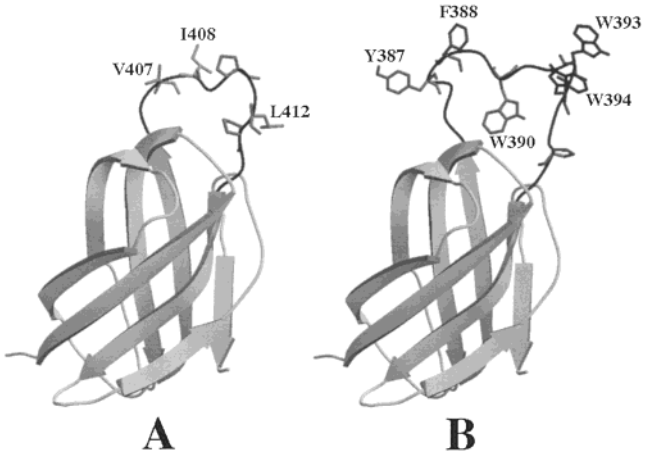

FIGURE 4: Ribbon models of C-terminal domains of HPL (A) and HPL-β5′LPL (B). A 3D model of the HPL-β5′LPL mutant was built using Turbo-Frodo as described in Experimental Procedures. The β5′ loop (black line) and its hydrophobic residues are shown on the top of the β-sandwich structure.

Table 3: Water Accessible Surfaces (Å^2) of the β5′ Loops of HPL and the HPL-β5′LPL Mutant[a]

	HPL	HPL-β5′LPL
charged residues	$C = 105$	$C = 203$
semipolar residues	$S = 284$	$S = 412$
hydrophobic residues	$H = 488$	$H = 914$
total surfaces	877	1529
HLB	0.80	0.67

[a] *C*, *S*, and *H* are the water accessible surfaces of charged residues (R, D, E, H, and K), semipolar residues (Q, G, N, C, S, and T), and hydrophobic residues (A, F, I, L, M, P, V, W, and Y), respectively. HLB is the hydrophilic/lipophilic balance and is defined by the $(C + S)/H$ ratio.

loaded onto a decylagarose column and eluted with a 10 mM Tris-HCl (pH 7.5) buffer containing either 0.1 M NaCl (Figure 5A) or 1 M NaCl (Figure 5B). In both cases, HPL was poorly retained on the column and was eluted with similar volumes of buffer. In contrast, HPL-β5′LPL was retained and its affinity for the hydrophobic matrix was increased by 1 M NaCl.

Effects of Bile Salts and Colipase on the Lipolytic Activity and Interfacial Binding of the HPL-β5′LPL Mutant Using Trioctanoin as a Substrate. We next investigated the activity and interfacial binding to trioctanoin of the HPL-β5′LPL mutant (10 μg per assay) in the presence or absence of colipase and at various sodium taurodeoxycholate (NaTDC) concentrations (Table 4). In the absence of bile salts and colipase, the interfacial binding of the HPL-β5′LPL mutant and HPL was very efficient but the specific activities were very low due to interfacial denaturation. In the presence of 0.5 mM NaTDC, a concentration at which the level of interfacial denaturation is reduced, HPL and HPL-β5′LPL exhibited nearly complete interfacial binding to trioctanoin and displayed maximum activity. When the NaTDC concentration was increased up to 4 mM, the two lipases were desorbed from the lipid−water interface and displayed no activity. The addition of a 5-fold molar excess of colipase increased the specific activity of HPL and of the HPL-β5′LPL mutant under all conditions. In the presence of 4 mM NaTDC, the addition of colipase restored the interfacial binding and the catalytic activity of HPL and of HPL-β5′LPL.

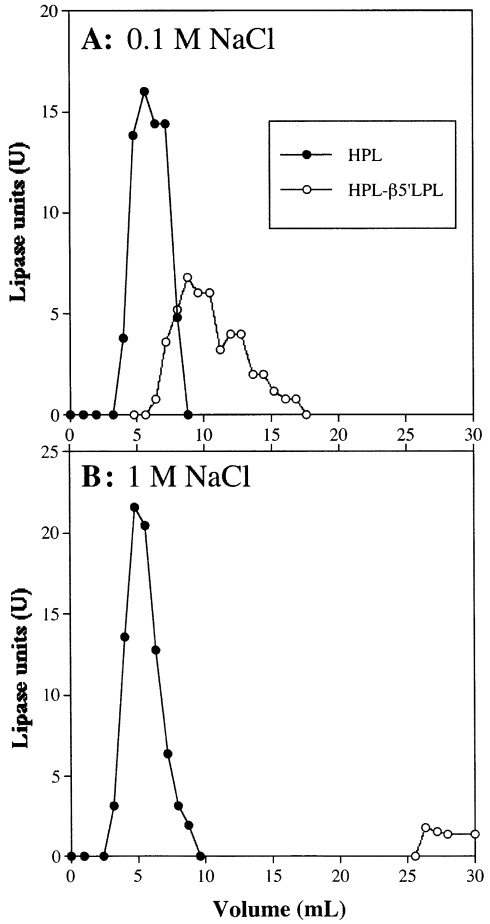

FIGURE 5: Comparison of the hydrophobic interactions of HPL and the HPL-$\beta5'$LPL mutant. Hydrophobic interaction chromatography was performed on a 2.5 mL decylagarose column equilibrated in Tris-HCl buffer, containing either 0.1 (A) or 1 M NaCl (B). After the lipase sample had been injected, the lipase activity was measured potentiometrically in all the fractions collected using the pHstat technique and tributyrin as the substrate (see Lipase Activity Measurements).

Since we measured the overall specific activity and the level of interfacial binding in each assay, it was possible to estimate the specific activity of the lipase bound at the interface (interfacial specific activity; see Table 4). By this analysis, the interfacial specific activities of the HPL-$\beta5'$LPL mutant and HPL differed significantly, even though they were on the same order of magnitude and varied similarly upon addition of colipase and bile salts. For instance, the maximum activity recorded with HPL at 0.5 mM NaTDC (9960 ± 145 U/mg) was 1.5-fold higher than the maximum activity recorded with the HPL-$\beta5'$LPL mutant (6543 ± 215 U/mg).

Similar experiments were performed with reduced amounts of lipase (1 vs 10 μg) in the assay. Whereas the results obtained with HPL were not significantly different, we observed that HPL-$\beta5'$LPL reactivation by colipase in the presence of 4 mM NaTDC only occurred after a lag period. The molar excess of colipase had to be increased from 5 to 50 to abolish the lag time and to obtain full reactivation of HPL-$\beta5'$LPL (data not shown). These results suggested that HPL-$\beta5'$LPL had a weaker affinity for colipase than HPL in the presence of bile salts.

Interactions of the HPL-$\beta5'$ LPL Mutant with Colipase. We next investigated the ability of the HPL-$\beta5'$LPL mutant to compete with an inactive HPL S152G mutant, for colipase binding. The experiments were performed in the presence of 4 mM NaTDC, a bile salt concentration at which colipase is absolutely required for measuring pancreatic lipase activity. We used a colipase to HPL molar ratio of 0.5 to work in a range where HPL activity varied linearly with the amount colipase (*29*), and lipase activity was therefore directly proportional to the formation of a 1:1 HPL−colipase complex. We showed in a previous study that HPL S152G, apart from being inactive, behaved like HPL in the presence of triocatanoin, bile salts, and colipase (*29*). We tested competition with two different experimental designs. In one, we preincubated equal amounts of the test lipase and HPL S152G with colipase before mixing them with trioctanoin (procedure A), and in the second, we added HPL S152G after starting trioctanoin hydrolysis with the same amount of the test lipase in the presence of colipase (procedure B). Addition of HPL S152G reduced HPL activity to 46.7 ± 4.6% (procedure A) and 41.7 ± 13.2% (procedure B; Table 5), indicating that HPL S152G had the same affinity for colipase as HPL since lipase activity was reduced by a factor of approximatively 2 in both experiments. In contrast, S152G reduced HPL-$\beta5'$LPL activity to 7.2 ± 1.9% (procedure A) and 13.8 ± 4.0% (procedure B), suggesting that HPL-$\beta5'$LPL has a lower affinity for colipase that does the S152G mutant.

Table 4: Effects of Bile Salts and Colipase on the Activity and Interfacial Binding of HPL and the HPL-$\beta5'$LPL Mutant[a]

protein	[NaTDC] (mM)	binding (%)	overall activity (U/mg)	interfacial specific activity (U/mg)[b]
HPL	0	97.8 ± 0.6	218 ± 10	226 ± 7
	0.5	92.2 ± 3.2	6228 ± 64	6759 ± 69
	4	1.0 ± 1.4	0	0
HPL and colipase	0	87.8 ± 2.4	1193 ± 70	1388 ± 79
	0.5	87.7 ± 1.6	8730 ± 127	9960 ± 145
	4	90.5 ± 2.3	8055 ± 318	8905 ± 351
HPL-$\beta5'$LPL	0	92.0 ± 1.3	250 ± 0	272 ± 0
	0.5	89.5 ± 5.8	4040 ± 735	4514 ± 821
	4	8.6 ± 14.8	0	0
HPL-$\beta5'$LPL and colipase	0	71.7 ± 1.7	2600 ± 500	3626 ± 697
	0.5	82.2 ± 1.3	5375 ± 177	6542 ± 215
	4	86.5 ± 7.0	4400 ± 566	5085 ± 654

[a] All the experiments were performed using 10 μg of HPL or HPL mutant in the assay (13 nM), with or without a 5-fold molar excess of colipase (10 μg per assay). [b] Since for each assay, the overall specific activity (international units per milligram of enzyme used in the assay) and the interfacial binding (fraction of enzyme bound at the interface) were measured, it was possible to estimate the specific activity of the lipase bound at the interface (interfacial specific activity).

Effects of BSA on the Lipolytic Activity and Interfacial Binding of the HPL-$\beta5'$LPL Mutant Using Trioctanoin as a Substrate. The activity and interfacial binding on trioctanoin of the HPL-$\beta5'$LPL mutant were investigated in the presence of various BSA concentrations (Figure 6 and Table 6). Just as we observed with bile salts, increasing BSA concentrations reduced the activity of both the HPL-$\beta5'$LPL mutant and HPL (Figure 6). This inhibition was related to the desorption of the lipases from the trioctanoin−water interface (Table 6). The mutation in the $\beta5'$ loop significantly affected the behavior of the HPL-$\beta5'$LPL mutant which displayed much higher activity than HPL at high BSA concentrations. At 200 nM BSA, HPL-$\beta5'$LPL retained 74% of its maximum overall activity versus 14% for HPL. This difference was mainly due to a more efficient binding of HPL-$\beta5'$LPL (50.2 ± 2.8%) than of HPL (10.1 ± 13.9%). HPL-$\beta5'$LPL still

Table 5: Competition between HPL S152G and HPL-β5′LPL Mutants for the Interaction with Colipase[a]

proteins (molar ratio)	lipase activity (U)	% of control
(A) Preincubation of the Lipases and Colipase before the Assay with Trioctanoin		
HPL/colipase (1:0.5), control	42.0 ± 1.3	100
HPL/HPL S152G/ colipase (1:1:0.5)	19.7 ± 2.5	46.7 ± 4.6
HPL-β5′LPL/ colipase (1:0.5), control	34.5 ± 0.7	100
HPL-β5′LPL/HPL S152G/colipase (1:1:0.5)	2.5 ± 0.7	7.2 ± 1.9
(B) Addition of the Second Lipase in the Course of Trioctanoin Hydrolysis		
HPL/colipase (1:0.5), control	42.0 ± 7.1	100
HPL/HPL S152G/ colipase (1:1:0.5)	18.0 ± 8.5	41.7 ± 13.2
HPL-β5′LPL/ colipase (1:0.5), control	31.5 ± 10.6	100
HPL-β5′LPL/HPL S152G/colipase (1:1:0.5)	4.1 ± 0.2	13.8 ± 4.0

[a] All the pHstat experiments were performed using trioctanoin as substrate, a NaTDC concentration of 4 mM, 10 μg of HPL (13 nM), 1 μg of colipase (6.5 nM; colipase:HPL molar ratio of 0.5), and 10 μg of HPL mutant (13 nM) when required. In procedure A, lipases and colipase were premixed before their injection into the pHstat vessel containing the trioctanoin emulsion. In procedure B, colipase and the first lipase (HPL or HPL-β5′LPL) were injected sequentially into the pHstat vessel containing the trioctanoin emulsion. The release of free fatty acids was monitored for 2 min, and then the second lipase was injected and the release of free fatty acids monitored for a further period of 2−3 min. One lipase unit (U) equals 1 μmol of free octanoic acid released per minute. Each assay was performed in triplicate.

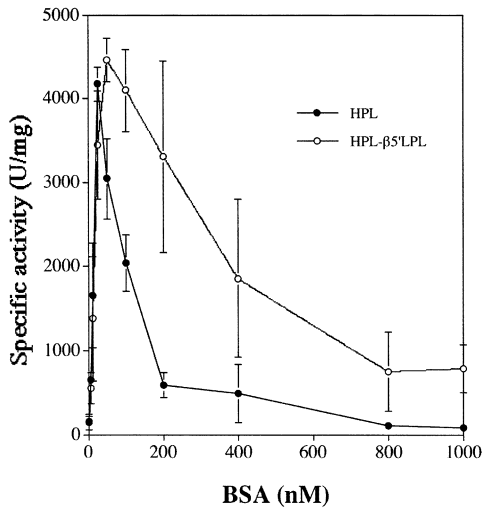

FIGURE 6: Effects of BSA on the hydolysis of trioctanoin by HPL and the HPL-β5′LPL mutant. Lipase activity was measured using the pHstat technique using trioctanoin as a substrate and various BSA concentrations (see Experimental Procedures).

displayed 18% of its maximum overall activity at 1000 nM BSA, whereas HPL was almost completely inhibited. At this BSA concentration, the β5′ loop mutation introduced into HPL-β5′LPL also had an effect on the interfacial specific activity which was 5-fold greater than that of HPL.

Adsorption and/or Penetration of HPL and the HPL-β5′LPL Mutant into a PC Monolayer. Comparisons were made between the HPL and HPL-β5′LPL mutant surface properties using the monolayer technique with monomolecular films of egg PC spread at the air−water interface. As in the case of HPL, egg PC is not a substrate for the HPL-β5′LPL mutant and the recorded variations in surface pressure therefore reflect only the lipase adsorption and/or penetration into the lipid monolayer. The maximum increase in the surface pressure ($\Delta\pi$) was plotted as a function of the initial surface pressure (π_i) of the egg PC monolayer (Figure 3). The critical surface pressure for penetration of HPL, i.e., the initial surface pressure beyond which no increase in the surface pressure occurs ($\Delta\pi = 0$) upon addition of the enzyme, was previously found to be 14.9 mN/m (*29*). On the other hand, HPL-β5′LPL was found to be a more penetrant protein that could induce a surface pressure increase of 6−7 mN/m when the initial surface pressure of the PC monolayer was 20 mN/m. The penetration capacity of HPL-β5′LPL was therefore between those of HPL and LPL, this latter enzyme being an extremely tensioactive protein that is able to penetrate into PC monolayers at surface pressures as high as 40 mN/m (*33*).

Table 6: Effects of BSA on the Activity and Interfacial Binding of HPL and the HPL-β5′LPL Mutant[a]

protein	[BSA] (nM)	binding (%)	overall activity (U/mg)	interfacial specific activity[b] (U/mg)
HPL	0	99.4 ± 0.4	140 ± 80	141 ± 80
	25	56.6 ± 4.3	4170 ± 209	7367 ± 369
	200	10.1 ± 13.9	592 ± 152	5861 ± 1505
	1000	9.2 ± 14.6	78 ± 18	848 ± 196
HPL-β5′LPL	0	91.7 ± 8.3	151 ± 96	165 ± 105
	50	51.6 ± 2.8	4457 ± 260	8637 ± 504
	200	50.2 ± 2.8	3307 ± 1137	6588 ± 2265
	1000	18.8 ± 1.3	786 ± 475	4181 ± 2526

[a] All the experiments were performed using 1 μg of HPL or HPL mutant in the assay. [b] Since for each assay, the overall specific activity (international units per milligram of enzyme used in the assay) and the interfacial binding (fraction of enzyme bound at the interface) were measured, it was possible to estimate the specific activity of the lipase bound at the interface (interfacial specific activity).

DISCUSSION

Since the description of the first lipase 3D structures, the lid domain controlling access to the active site has been a major target for structure−function studies aimed at understanding lipase−lipid interactions. The opening of the lid domain generates a large hydrophobic surface around the lipase active site, and it was proposed that this surface was the main site of interaction with the lipid−water interface (*2*, *34*). In the case of pancreatic lipase, this hypothesis was challenged by mutagenesis of the lid domain. An HPL mutant in which the lid was deleted could bind to trioctanoin emulsions and could penetrate into PC monolayers (*29*). Even though the lid deletion does not totally suppress the hydrophobic surface around the active site of HPL, these experiments suggested that some other structural features might be essential for the interfacial binding of HPL. At the same time, several observations indicated that the β5′ loop of the HPL C-terminal domain interacts with micelles (*14*, *35*) and may interact directly with the lipid−water interface (*9*). The importance of a homologous loop in lipoprotein lipase had already been recognized for the interaction with lipoproteins (*11*, *12*).

In this study, we first demonstrated that the isolated HPL C-terminal domain could efficiently bind to a triglyceride−water interface in the absence of bile salts (Table 2) and

could also adsorb and penetrate into a phospholipid monolayer with a criticical surface pressure of penetration similar to that of HPL (~15 mN/m; Figure 3). Under this critical surface pressure, the increase in surface pressure induced by the penetration of C-HPL into the phospholipid monolayer was lower than that recorded with HPL, probably because of the reduced size of C-HPL (12 kDa, vs 50 kDa for HPL). In contrast, the N-terminal domain of HPL did not bind efficiently to a triglyceride−water interface, even in the absence of amphiphiles such as bile salts (Table 2), confirming previous observations with truncated HPL mutants (*36*). The results of all the experiments described here, performed in the absence of colipase, support an absolute requirement of the C-terminal domain for interfacial binding of HPL. The absolute requirement for the C-terminal domain provides an explaination for why N-HPL does not display any significant activity on an insoluble triglyceride substrate (*9*, *37*).

The presence of a C-terminal lipid binding domain clearly distinguishes PL from gastric lipase and several microbial lipases which are globular proteins with a single structural domain (*38*, *39*). These lipases share common structural features with the N-terminal catalytic domain of PL (the α/β hydrolase fold and a lid controlling the access to the active site), but they can bind to an oil−water interface and hydrolyze triglyceride emulsions. Comparative structural studies could improve our understanding of why these lipases do not require an additional lipid binding site.

Our results show that the structural similarities noted between the C-terminal domain of PL and C2 domains of other proteins (*19*) confer similar functions on these proteins. They all interact with lipids. Another interesting similarity between C2 domains and the C-terminal domain of HPL is the presence of an exposed hydrophobic loop (CBR3) with the same topology as the β5′ loop of HPL (*19*). In the case of cPLA2, fluorescence spectroscopy (*40*) and EPR studies (*41*) have shown that the hydrophobic residues (Y96, V97, and M98) of CBR3 penetrate into the phospholipid bilayer of liposomes. Site-directed mutagenesis of these residues impairs the binding the cPLA2 C2 domain onto liposomes, as well as the in vivo translocation of PLA2 to cellular membranes (*40*). We investigated whether the hydrophobicity of the β5′ loop was also important for the interfacial binding and activity of HPL. The substitution of the HPL β5′ loop with that of LPL (HPL-β5′LPL mutant) clearly increased the overall hydrophobicity of the protein as shown by hydrophobic interaction chromatography (Figure 5), and as predicted from modeling studies (Table 3). Using monolayer experiments, the HPL-β5′LPL mutant was also found to be a more tensioactive protein than HPL (Figure 3). The higher capacity of HPL-β5′LPL for penetration into a phospholipid monolayer probably resulted from the presence of several polar-aromatic residues in the β5′ loop (Figure 2) which have a specific affinity for polar−apolar interfaces (*42*).

Like HPL, the HPL-β5′LPL mutant could bind very efficiently to an oil−water interface (pure trioctanoin) in the absence of any other tensioactive molecule and in the presence of 0.5 mM bile salts (Table 4). Under these conditions, addition of colipase increased the rate of turnover of the mutant and HPL at the interface but had no significant impact on their interfacial binding (Table 4). Since bile salts are known to compete with HPL for interfacial binding (*29*, *43*, *44*), we increased the bile salt concentration and observed that the inactivation by bile salts and the interfacial binding of HPL-β5′LPL mutant and HPL were similar (Table 4).

The latter results prompted us to investigate the effects of other amphiphilic molecules such as BSA which is also known to compete with HPL for interfacial binding but has a lower tensioactivity than bile salts. Borgström and Erlanson have shown that porcine pancreatic lipase was protected against surface denaturation by BSA at low concentrations (10^{-7} M), but that higher BSA concentrations decreased the level of lipase binding at the oil−water interface and therefore reduced the enzyme activity (*45*). Similar results can be obtained with other proteins such as β-lactoglobulin, myoglobin, and ovalbumin (*45*−*47*). We studied the effects of BSA on the activity (Figure 6) and binding (Table 6) of HPL and the HPL-β5′LPL mutant. In accord with Borgström and Erlanson's findings, low concentrations of BSA (25 nM for HPL and 50 nM for HPL-β5′LPL) stimulated maximum lipase activity and lipase activity decreased when the BSA concentration was increased. The inactivation and desorption of HPL-β5′LPL required a much higher concentration of BSA than in the case of HPL (Figure 6). Again, these observations support the importance of the β5′ loop hydrophobicity in the interaction with the lipid−water interface in the presence of proteins. Increasing the β5′ loop hydrophobicity increases the affinity of HPL for the interface versus that of competitive proteins such as BSA. It is worth recalling here that Borgström and Erlanson already proposed that the binding of lipase to its substrate interface may be caused by "a specific binding of a localized hydrophobic site on the protein that does not give the lipase an overall hydrophobic character" (*45*). Hydrophobic interaction chromatography (Figure 5) confirms that HPL does not display an overall hydrophobic character.

Since the β5′ loop is known to interact with detergent micelles in the crystal structure of the porcine PL−colipase complex (*14*), we investigated the role of the β5′ loop in a more complex system in which a trioctanoin emulsion was formed in the presence of a micellar concentration of bile salts (4 mM NaTDC), with or without colipase. Like HPL, the HPL-β5′LPL mutant was inactivated and desorbed from the interface in the absence of colipase (Table 4). Addition of colipase reactivated HPL-β5′LPL only after a lag period. These results first suggested that the interfacial binding of the HPL-β5′LPL mutant−colipase complex was impaired by the β5′ loop mutation. Competition experiments to test the binding of the lipases to colipase showed that the apparent affinity for colipase was reduced in the case of HPL-β5′LPL as compared to HPL. Since the β5′ loop does not interact directly with colipase, one hypothesis developed to explain these results could be the existence of a lipase−colipase−bile salt complex that stabilizes the lipase−colipase interaction (*14*, *35*, *48*). The β5′ loop mutation might impair the lipase−bile salt interactions and, indirectly, might reduce the affinity of colipase for the lipase. Recent articles report the existence of a ternary PL−colipase−bile salt micelle complex in solution (*35*, *48*), and it has been proposed that bile salt micelles (*14*) are required to direct the adsorption of the PL−colipase complex toward the oil−water interface. It is, however, difficult to imagine a specific ternary interaction between two well-defined molecular entities (PL and colipase) and a micelle constituted by molecules that dissociate at a millisecond rate. In fact, the "shuttle" function of bile

salt micelles for driving the PL−colipase complex toward the oil−water interface has been extrapolated from experiments performed with bile (*49*). Bile not only contains bile salts but also contains large amounts of phospholipids and cholesterol. All these molecules form large lipoproteins when they are mixed with PL and colipase.

Another hypothesis that cannot be excluded by the results of the competition experiments is that the mutation of the $\beta5'$ loop impairs the interfacial binding of the HPL-$\beta5'$LPL mutant−colipase complex in the presence of bile salts, but not the affinity of colipase for the HPL-$\beta5'$LPL mutant in the bulk phase. In this scenario, the stronger affinity of the HPL S152G−colipase complex for the interface may cause colipase to accumulate at the interface, thereby decreasing the concentration of colipase in solution. The drop in colipase concentration in solution would induce the dissociation of the HPL-$\beta5'$LPL−colipase complex and, consequently, decrease the amount of the HPL-$\beta5'$LPL−colipase complex at the interface. The affinity of HPL-$\beta5'$LPL for colipase in solution remains to be investigated in the presence and absence of bile salts.

A final hypothesis developed to explain the apparent low affinity of HPL-$\beta5'$LPL for colipase is that the LPL $\beta5'$ loop could a hinder binding between HPL-$\beta5'$LPL and colipase. The larger LPL $\beta5'$ loop resides near the binding sites of colipase and could sterically hinder the binding of the mutant lipase and colipase. Alternatively, the introduction of the LPL $\beta5'$ loop into HPL could cause enough local perturbation of the protein structure near the colipase binding site that binding is inhibited even there is no gross alteration of the HPL structure in the mutant.

Some Considerations about the Role of the $\beta5'$ Loop in LPL. As shown by the results obtained with the HPL-$\beta5'$LPL mutant, the LPL $\beta5'$ loop increases the extent of penetration of lipase into a monolayer of phospholipids (Figure 6) and increases the level of lipase adsorption at the lipid−water interface in the presence of proteins (Figure 3). The LPL $\beta5'$ loop is therefore tailored for an optimal interaction with the surface of triglyceride-rich lipoproteins (VLDL and chylomicrons) containing phospholipids and apoproteins. Like LPL (*33*), the HPL-$\beta5'$LPL mutant is able to penetrate into PC monolayers at high surface pressures. These observations suggest a major contribution of the $\beta5'$ loop in the interaction of LPL with its substrate and support previous reports (*11*, *12*).

ACKNOWLEDGMENT

Our thanks are due to Jacques Bonicel (IBSM Marseille, Marseille, France) for N-terminal sequence analysis and for mass spectrometry analysis of the HPL mutants, to Josiane De Caro for her generous gift of the HPL C-terminal domain, to Dr. Alain de Caro for his help and advice in setting up the ELISA procedures and for his generous gift of monoclonal antibodies, and to Dr. Jessica Blanc for revising the English. We are grateful to Dr. Robert Verger and Prof. Louis Sarda for their careful critical reading of the manuscript.

REFERENCES

1. Winkler, F. K., d'Arcy, A., and Hunziker, W. (1990) *Nature 343*, 771−774.
2. van Tilbeurgh, H., Egloff, M.-P., Martinez, C., Rugani, N., Verger, R., and Cambillau, C. (1993) *Nature 362*, 814−820.
3. van Tilbeurgh, H., Sarda, L., Verger, R., and Cambillau, C. (1992) *Nature 359*, 159−162.
4. van Tilbeurgh, H., Roussel, A., Lalouel, J. M., and Cambillau, C. (1994) *J. Biol. Chem. 269*, 4626−4633.
5. Hirata, K. I., Dichek, H. L., Cioffi, J. A., Choi, S. Y., Leeper, N. J., Quintana, L., Kronmal, G. S., Cooper, A. D., and Quertermous, T. (1999) *J. Biol. Chem. 274*, 14170−14175.
6. Sato, T., Aoki, J., Nagai, Y., Dohmae, N., Takio, K., Doi, T., Arai, H., and Inoue, K. (1997) *J. Biol. Chem. 272*, 2192−2198.
7. Roussel, A., de Caro, J., Bezzine, S., Gastinel, L., de Caro, A., Carriere, F., Leydier, S., Verger, R., and Cambillau, C. (1998) *Proteins 32*, 523−531.
8. Roussel, A., Yang, Y., Ferrato, F., Verger, R., Cambillau, C., and Lowe, M. (1998) *J. Biol. Chem. 273* (48), 32121−32128.
9. Bezzine, S., Carrière, F., De Caro, J., Verger, R., and De Caro, A. (1998) *Biochemistry 37*, 11846−11855.
10. Liu, M. S., Ma, Y., Hayden, M. R., and Brunzell, J. D. (1992) *Biochim. Biophys. Acta 1128*, 113−115.
11. Lookene, A., Groot, N. B., Kastelein, J. J. P., Olivecrona, G., and Bruin, T. (1997) *J. Biol. Chem. 272*, 766−772.
12. Lookene, A., and Bengtsson-Olivecrona, G. (1993) *Eur. J. Biochem. 213*, 185−194.
13. Carrière, F., Thirstrup, K., Hjorth, S., Ferrato, F., Withers-Martinez, C., Cambillau, C., Boel, E., Thim, L., and Verger, R. (1997) *Biochemistry 36*, 239−248.
14. Hermoso, J., Pignol, D., Penel, S., Roth, M., Chapus, C., and Fontecilla-Camps, J. C. (1997) *EMBO J. 16*, 5531−5536.
15. Gillmor, S. A., Villasenor, A., Fletterick, R., Sigal, E., and Browner, M. F. (1997) *Nat. Struct. Biol. 4*, 1003−1009.
16. Naylor, C. E., Eaton, J. T., Howells, A., Justin, N., Moss, D. S., Titball, R. W., and Basak, A. K. (1998) *Nat. Struct. Biol. 5*, 738−746.
17. Nalefski, E. A., and Falke, J. J. (1996) *Protein Sci. 5*, 2375−2390.
18. Rizo, J., and Südhof, T. C. (1998) *J. Biol. Chem. 273*, 15879−15882.
19. Chahinian, H., Sias, B., and Carrière, F. (2000) *Curr. Protein Pept. Sci. 1*, 91−103.
20. Dessen, A., Tang, J., Schmidt, H., Stahl, M., Clark, J. D., Seehra, J., and Somers, W. S. (1999) *Cell 97*, 349−360.
21. Chen, X. S., and Funk, C. D. (2001) *J. Biol. Chem. 276*, 811−818.
22. Thirstrup, K., Carrière, F., Hjorth, S., Rasmussen, P. B., Wöldike, H., Nielsen, P. F., and Thim, L. (1993) *FEBS Lett. 327*, 79−84.
23. Lowe, M. E., Rosenblum, J. L., and Strauss, A. W. (1989) *J. Biol. Chem. 264*, 20042−20048.
24. Sambrook, J., Fritsch, E. F., and Maniatis, T. (1989) *Molecular cloning. A laboratoty manual*, 2nd ed., Cold Spring Harbor Laboratory Press, Plainview, NY.
25. Higuchi, R. (1992) in *PCR Technology: Principles and Applications for DNA Amplification* (Erlich, H. A., Ed.) pp 61−70, W. H. Freeman and Co., New York.
26. Bezzine, S., Ferrato, F., Lopez, V., De Caro, A., Verger, R., and Carrière, F. (1999) in *Lipase and Phospholipase Protocols* (Doolitle, M. H., and Reue, K., Eds.) pp 187−202, Humana Press, Totowa, NJ.
27. O'Reilly, D. R., Miller, L. K., and Luckow, V. A. (1994) *Baculovirus expression vectors: a laboratory manual*, Oxford University Press, New York.
28. Laemmli, U. K. (1970) *Nature 227*, 680−685.
29. Bezzine, S., Ferrato, F., Ivanova, M. G., Lopez, V., Verger, R., and Carriere, F. (1999) *Biochemistry 38*, 5499−5510.
30. De Caro, A., Bezzine, S., Lopez, V., Aoubala, M., Daniel, C., Verger, R., and Carrière, F. (1999) in *Lipase and Phospholipase Protocols* (Doolitle, M. H., and Reue, K., Eds.) pp 239−256, Humana Press, Totowa, NJ.
31. Roussel, A., and Cambillau, C. (1989) in *Silicon Graphics Geometry Partners Directory* (Graphics, S., Ed.) pp 77−78, Silicon Graphics, Mountain View, CA.
32. Kabsch, W., and Sander, C. (1983) *Biopolymers 22*, 2577−2637.
33. Vainio, P., Virtanen, J. A., Kinnunen, P. K. J., Voyta, J. C., Smith, L. C., Gotto, J., Antonio M., Sparrow, J. T., Pattus, F., and Verger, R. (1983) *Biochemistry 22*, 2270−2275.
34. Brzozowski, A. M., Derewenda, U., Derewenda, Z. S., Dodson, G. G., Lawson, D. M., Turkenburg, J. P., Bjorkling, F., Huge-Jensen, B., Patkar, S. A., and Thim, L. (1991) *Nature 351*, 491−494.

35. Pignol, D., Ayvazian, L., Kerfelec, B., Timmins, P., Crenon, I., Hermoso, J., Fontecilla-Camps, J. C., and Chapus, C. (2000) *J. Biol. Chem. 275*, 4220−4224.
36. Jennens, M. L., and Lowe, M. E. (1995) *J. Lipid Res. 36*, 1029−1036.
37. Ayvazian, L., Crenon, I., Granon, S., Chapus, C., and Kerfelec, B. (1996) *Protein Eng. 9*, 707−711.
38. Roussel, A., Canaan, S., Egloff, M. P., Riviere, M., Dupuis, L., Verger, R., and Cambillau, C. (1999) *J. Biol. Chem. 274*, 16995−17002.
39. Derewenda, Z. S., and Sharp, A. M. (1993) *Trends Biochem. Sci. 18*, 20−25.
40. Perisic, O., Paterson, H. F., Mosedale, G., Lara-Gonzalez, S., and Williams, R. L. (1999) *J. Biol. Chem. 274*, 14979−14987.
41. Ball, A., Nielsen, R., Gelb, M. H., and Robinson, B. H. (1999) *Proc. Natl. Acad. Sci. U.S.A. 96*, 6637−6642.
42. Killian, J. A., and von Heijne, G. (2000) *Trends Biochem. Sci. 25*, 429−434.
43. Momsen, W. E., and Brockmann, H. L. (1976) *J. Biol. Chem. 251*, 384−388.
44. Borgström, B. (1975) *J. Lipid Res. 16*, 411−417.
45. Borgström, B., and Erlanson, C. (1978) *Gastroenterology 75*, 382−386.
46. Gargouri, Y., Julien, R., Sugihara, A., Verger, R., and Sarda, L. (1984) *Biochim. Biophys. Acta 795*, 326−331.
47. Gargouri, Y., Piéroni, G., Rivière, C., Sarda, L., and Verger, R. (1986) *Biochemistry 25*, 1733−1738.
48. Ayvazian, L., Kerfelec, B., Granon, S., Foglizzo, E., Crenon, I., Dubois, C., and Chapus, C. (2001) *J. Biol. Chem. 276*, 14014−14018.
49. Lairon, D., Nalbone, G., Lafont, H., Leonardi, J., Domingo, N., Hauton, J.-C., and Verger, R. (1978) *Biochemistry 17*, 5263−5269.
50. Nicholls, A. J. (1993) Ph.D. Thesis, Columbia University, New York.
51. Kraulis, P. (1991) *J. Appl. Crystallogr. 24*, 946−950.
52. Merrit, E. A., and Murphy, M. E. P. (1994) *Acta Crystallogr. D50*, 869−873.

BI0257944